Cyclic numerical analyses of Noto Cathedral: soil-structure interaction modelling

Claudio di Prisco,* Maria Rossella Massimino,** Michele Maugeri,** Massimo Nicolosi,** Roberto Nova*

Summary

In a country like Italy, characterised by high seismic hazard and vast cultural heritage, the protection of historical monuments against the effects of seismic events is of great importance. The seismic safety of these structures is usually evaluated by disregarding soil-structure interaction, that can instead play an important role.

The aim of this paper consists in introducing a simplified approach for taking numerically into account this aspect. Soil-structure interaction in cyclic conditions is taken into consideration by interpreting the foundation system as a macro-element, whose mechanical response is described by an elasto-hypoplastic constitutive relationship. The model allows for both isotropic and kinematic hardening and its constitutive parameters are calibrated with reference to granular soils. It is shown that the numerical implementation of this model in a standard FEM code allows the mechanical response of a 2-D cross section of Noto Cathedral to be realistically reproduced. In particular the beneficial effect of tie rods connecting footings is highlighted. It is further shown that the cyclic accumulation of vertical settlements under the action of strong earthquakes may eventually lead to footing failure due to vertical force redistribution.

1. Introduction

The seismic retrofitting of monuments and ancient buildings represents a problem of high interest in Italy. In fact, the number of buildings of great historical and architectonical importance situated in this country, which are exposed to a high seismic hazard, is actually very large. This is particularly true, for instance, for the Eastern area of Sicily, near to the Ibleo-Maltese fault [Bottari *et al.*, 2003], where a large number of seismic events of dramatic intensity occurred in the past (1169, 1542, 1693). During the last one, the "Santa Lucia" earthquake of December 13th 1990, the Cathedral of Noto, which represents one of the most famous examples of Sicilian Baroque, suffered considerable damage. Extensive cracks appeared in the columns during and immediately after the earthquake, whereas the collapse of the five right-side columns of the central nave, of part of the dome and of the covering of the nave took place later on March 13th 1996 (Fig. 1). The subsequent reconstruction design needed the seismic retrofitting of the whole structure. For this reason, in the last decade, various studies have been performed in order to evaluate the local geotechnical seismic hazard [Campoccia and Massimino., 2003] and to develop a site-dependent design spectrum [Massimino and Maugeri, 2003a].

In the literature, many studies testify the important effects of soil-structure interaction on the static and dynamic response of structures [Poulos, 1975; Mylonakis and Gazetas, 2000; Prakash, 2004]. Numerical finite element analyses of the structure and of the soil beneath it have been already performed for the Cathedral by two of the authors [Massimino and Maugeri, 2003b; Massimino *et al.*, 2004].

The aim of this paper consists in investigating the soil-structure interaction for Noto Cathedral by means of a FEM numerical code under cyclic loading. 2-D numerical analyses have been performed by taking into account a representative cross-section of the Cathedral. This section is assumed to be subjected both to pseudo-static and cyclic horizontal forces. The amplitude of the horizontal forces applied to the nodes depends on the structural element masses. The foundations are considered to be rigid and the soil-structure interaction problem is modelled by means of the macro-element concept [Montrasio and Nova, 1988]. The elasto-hypoplastic SFCM constitutive model [di Prisco *et al.*, 2003], which represents an evolution of the Nova-Montrasio [1991] constitutive law, is used to this goal. This model accounts for isotropic and kinematic hardening and it is particularly suitable for cyclic loading conditions. In particular it can describe the progressive accumulation of vertical displacements under cyclic loads. These can have a relevant influence on the redistribution of vertical forces and eventually lead to foundation failure.

* Department of Structural Engineering, Politecnico di Milano, Milan (Italy)

** Department of Civil and Environmental Engineering, University of Catania, Catania (Italy)

2. The elasto-hypoplastic SFCM constitutive model

In order to define an appropriate constitutive relationship for the soil-footing interaction, it is convenient to introduce the concept of the generalised stresses acting on the foundation. If we analyse a shallow strip foundation of width B, subjected to an inclined and eccentric load, we can define as generalised stresses the equivalent loads applied to the foundation centre of mass: the vertical force V, the horizontal force H and the overturning moment M. According to the experimental results obtained in the last decades [BUTTERFIELD *and* TICOV 1979; NOVA *and* MONTRASIO, 1991; BUTTERFIELD *et al.*, 1993], the shape of the failure locus in the associated generalised stress space (V, H, M/B) seems to be conveniently fitted by the following expression:

$$H^2+\left(\frac{M}{B}\right)^2-V^2\left(\frac{V_M-V}{V_M}\right)^{2\beta}=0 \qquad (1)$$

where β is a constitutive parameter equal to 0.95 and V_M is the bearing capacity of the foundation for M=H=0.

Starting from such a point, by assuming the foundation and the soil underneath as a unique system called "macro-element", Nova-Montrasio [1991] conceived a rigid-plastic non-associated constitutive model with isotropic strain hardening. The yield locus, similar in shape to the failure locus, grows in size with increasing generalised strains (vertical and horizontal displacements and foundation rotation) until failure is achieved. A generalised constitutive law between generalised stresses and generalised strains can be defined and the mechanical response of a strip foundation on a homogeneous sand stratum along monotonic generalised stress paths can be reproduced. Because of the assumed isotropic strain hardening, however, the model can not simulate the accumulation of plastic generalised strains during cyclic loading. To overcome this limitation, DI PRISCO *et al.* [1998] and DI PRISCO *et al.* [2003] developed the SFCM model, which will be briefly outlined in the following paragraph.

2.1. Mathematical formulation of the modified SFCM constitutive model

By following the NOVA-MONTRASIO [1991] constitutive model, in order to evaluate the irreversible displacements, we define one dimensionless vector Q for the generalised stresses, and one dimensionless vector q, for the associated irreversible generalised strains. These vectors are defined as:

$$\underline{Q}=\begin{Bmatrix}\xi\\ h\\ m\end{Bmatrix}=\frac{1}{V_M}\begin{Bmatrix}V\\ H/\mu\\ M/(\psi\cdot B)\end{Bmatrix} \quad \underline{q}=\begin{Bmatrix}\eta\\ \varepsilon\\ \zeta\end{Bmatrix}=V_M\begin{Bmatrix}v^p\\ \mu\cdot u^p\\ \psi\cdot(B\cdot\theta^p)\end{Bmatrix} \qquad (2)$$

where v^p and u^p are the plastic displacements in the vertical and horizontal directions, respectively, while θ^p is the plastic footing rotation. μ and ψ are two constitutive parameters governing the shape of both the failure locus and the yield locus. For embedded foundations, the aforementioned authors [MONTRASIO and NOVA, 1997] suggest for the evaluation of these parameters the following empirical relations:

$$\mu=tg(\delta)+0.72\cdot\frac{D}{B} \qquad (3)$$

$$\psi=0.35+0.3\frac{D}{B} \qquad (4)$$

where δ is the soil-footing interface friction angle, while D is the foundation embedment.

The loading function f in the 3-D space ξ-h-m is defined as follows:

$$f(\underline{Q},\rho_c)=h^2+m^2-\xi^2\left[1-\left(\frac{\xi}{\rho_c}\right)\right]^{2\beta}=0 \qquad (5)$$

where ρ_c is the hardening parameter, which controls the size of the domain. Its evolution is governed by an appropriate hardening rule:

$$d\rho_c(d\underline{q})=(1-\rho_c)\frac{R_0}{V_m^2}\left[d\eta^*+\frac{\alpha|d\varepsilon^*|}{\mu}+\frac{\overline{\gamma}\,|d\zeta^*|}{\psi}\right], \qquad (6)$$

where $d\eta^*$, $d\varepsilon^*$, $d\zeta^*$ are the components of the vector dq^*, whose meaning will be introduced here below and α, $\overline{\gamma}$ and R_0 are constitutive parameters. $\rho_c=1$ is an asymptotic value for the hardening parameter: when such a condition is satisfied, the yield function coincides with the failure locus. Moreover, the mechanical meaning of the star symbols in Eq. (6) will be outlined in the following of this section, after having described the hypoplastic extension of the model.

R_0 describes the initial stiffness of the load-displacement curve when H = M = 0, while α and γ^* influence the system stiffness respectively when H and M are not nil.

The Nova-Montrasio [1991] model assumes a non-associated flow rule and the generalised plastic strain rate vector is governed by the plastic potential g:

$$\underline{g}(\underline{Q},\rho_g)=\lambda^2\cdot h^2+\chi^2\cdot m^2-\xi^2\cdot\left[1-\left(\frac{\xi}{\rho_g}\right)\right]^{2\cdot\beta}=0 \qquad (7)$$

where λ and χ are two additional parameters, while ρ_g is a dummy variable.

To simulate the mechanical response of the system during cyclic loading, the SFCM model assumes that even within the previously defined yield locus,

Fig. 1 – View of the damage occurred at Noto Cathedral on March 13th 1996.
Fig. 1 – Vista dei danni verificatisi nella Cattedrale di Noto il 13 marzo 1996.

plastic generalised strains may occur. To define the generalised strain rate vector when $f<0$, a particular hypoplastic approach was chosen. An additional inner reversible locus $f_2 = 0$ (Fig. 2) is introduced: its size is very small if it is compared with f. Its expression is not here reported for the sake of brevity. A mapping rule (Fig. 2) associates each stress point P_i on the inside of the boundary surface f belonging to the boundary of the reversible locus to a corresponding *image point* ($I_{i)}$ on $f=0$.

The flow rule is modified as follows:

$$d\underline{q}=\Lambda(\underline{Q}_I)\underline{\underline{\Phi}}(\tilde{\delta})\frac{\partial g}{\partial \underline{Q}}(\underline{Q}_I), \tag{8}$$

where both the plastic multiplier Λ and the gradient to the plastic potential are calculated in the image point I_i. $\underline{\underline{\Phi}}(\tilde{\delta})$ is a diagonal matrix function of a variable $\tilde{\delta}$, which represents, in the dimensionless stress space, the distance between P_i and the corresponding image point I_i (Fig. 2). The role of $\underline{\underline{\Phi}}(\tilde{\delta})$ is that of a weight function: the larger is $\tilde{\delta}$ the smaller is the value of the diagonal terms of $\underline{\underline{\Phi}}$ and the smaller are the calculated plastic strains. Each diagonal term Φ_{ii} is expressed as:

$$\Phi_{ii}=e^{-\left(\tilde{\xi}_i\sqrt{\frac{\tilde{\delta}\rho_c}{\xi}}\right)}, \tag{9}$$

where $\tilde{\xi}_i$ are constitutive parameters. In all the numerical simulations illustrated in the following $\tilde{\xi}_2=\tilde{\xi}_3$. This constraint has been empirically derived by numerically simulating large scale test results [DI PRISCO *et al.*, 2003].

When $\tilde{\delta} = 0$, i.e. when point I coincides with point P of Fig.2, $d\underline{q}\equiv d\underline{q}^*$, whereas when $\tilde{\delta}>0$, $d\underline{q}^*=0$. This means [see Eq. (6)] that the yield locus evolves if and only if the generalised state of stress image point belongs to the yield locus $f=0$.

By comparing Eq. (9) to those introduced in DI PRISCO *et al.* [2003] and by considering the definition of $\tilde{\delta}$, it is evident that the FEM analyses illustrated in the following were performed by implementing a simplified version of the cited model. Such a choice is justified both by the type of cyclic loading applied and by the number of loading cycles. In fact, under these conditions the ratcheting phenomenon can be disregarded and the anisotropic hardening not taken into consideration.

Finally, we must observe that, in order to define the complete constitutive relationship, the irreversible displacement rates here above introduced are to be added to the reversible displace-

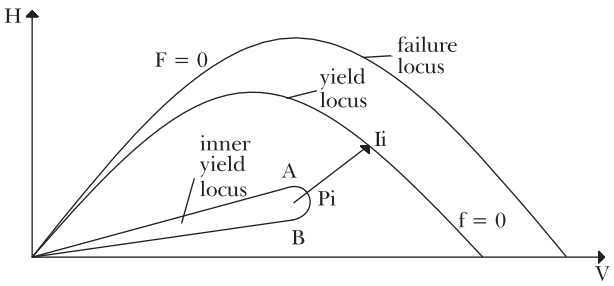

Fig. 2 – Bounding surface and domain of reversibility: current stress P_i and current image point I_i [after DI PRISCO *et al.*, 2003].
Fig. 2 – Superficie di plasticizzazione e dominio di reversibilità: sforzo corrente P_i e punto immagine corrente I_i [da DI PRISCO et al., *2003].*

ment increments. The terms of the elastic diagonal matrix employed to evaluate these latter are presented in section 3.1.

3. FEM analyses

A 3-D analysis of the soil-structure interaction by means of FEM codes for Noto Cathedral is very complex and could also lead to results not easily understandable. For this reason in the present paper a 2-D analysis is performed considering a significative π section across the nave (Fig. 3). In this paragraph, both the structural schematisation and the soil-foundation interaction are outlined. As far as the former point is concerned, the work of Massimino and Maugeri [2003b] will be briefly summarised, while for the latter one, the values of the constitutive parameters employed to perform the numerical simulations will be given and discussed.

3.1. Structural schematisation

The section of Figure 3 taken into consideration has been first schematised as a frame structure characterised by 44 1-D elements and 43 nodes (Fig. 4).

The geometrical characteristics of the retrofitted foundations (Figs. 5 and 6) are reported in Table I [Massimino and Maugeri, 2003b].

As far as the foundation retrofitting is concerned, to connect the column footings each other along the longitudinal direction, and to the external wall foundations along the transversal direction, inverted arches have been introduced. Moreover, all the foundation elements have been connected by tie rods (Fig. 5). In this paper, both the tie rods connecting the foundation nodes 1, 11, 33 and 43 of the chosen π section and those connecting the superstructure nodes 5-15 and 29-39 are taken into consideration. The mechanical characteristics of the designed Dywidag tie rods and the steel unit weight γ_f are reported in Table II.

The mechanical behaviour of these tie rods is assumed to be linear-elastic: more details can be found in Massimino *et al.* [2004]. In Figure 7, the new 2-D scheme of the complete structure characterised by 60 1-D elements and the 54 nodes is illustrated.

The 44 masonry structural elements are characterized by six different sections, as is reported in Table III. For the sake of simplicity, the mechanical behav-

Tab. I – Foundation geometrical characteristics of the chosen cross section [after Massimino and Maugeri, 2003b].
Tab. I – Caratteristiche geometriche delle fondazioni della sezione trasversale considerata [da Massimino and Maugeri, 2003b].

Assumed Foundation Characteristics			
Node	B_1 (m)	B_2 (m)	D (m)
1	5.30	8.00	1.25
11	4.30	7.00	2.50
33	4.30	7.00	2.50

Tab. II – Mechanical characteristics of the employed Dywidag tie rods.
Tab. II – Caratteristiche meccaniche delle barre Dywidag adottate.

ϕ(mm)	E(MPa)	v	γ_f(kN/m^3)
30	206000	0.17	77

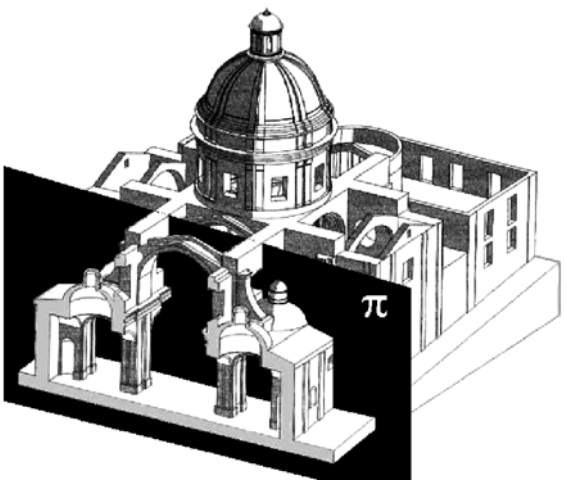

Fig. 3 – Representative section across the nave chosen for the 2-D FEM analyses.
Fig. 3 – Sezione trasversale π scelta per le analisi numeriche.

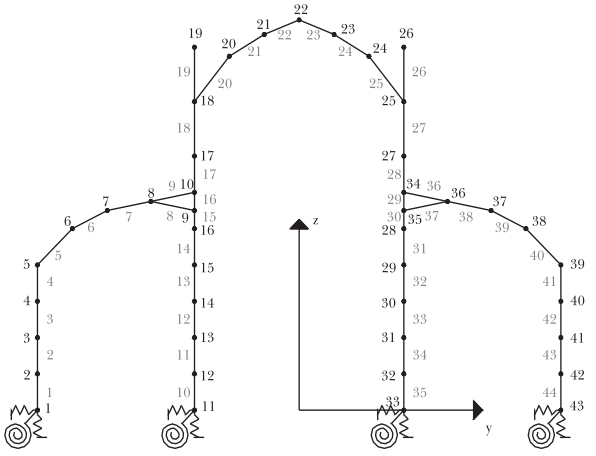

Fig. 4 – Plane structural scheme of Noto Cathedral employed for the FEM analyses [after Massimino and Maugeri, 2003b].
Fig. 4 – Schema strutturale piano della Cattedrale di Noto usato per le analisi FEM [da Massimino and Maugeri, 2003b].

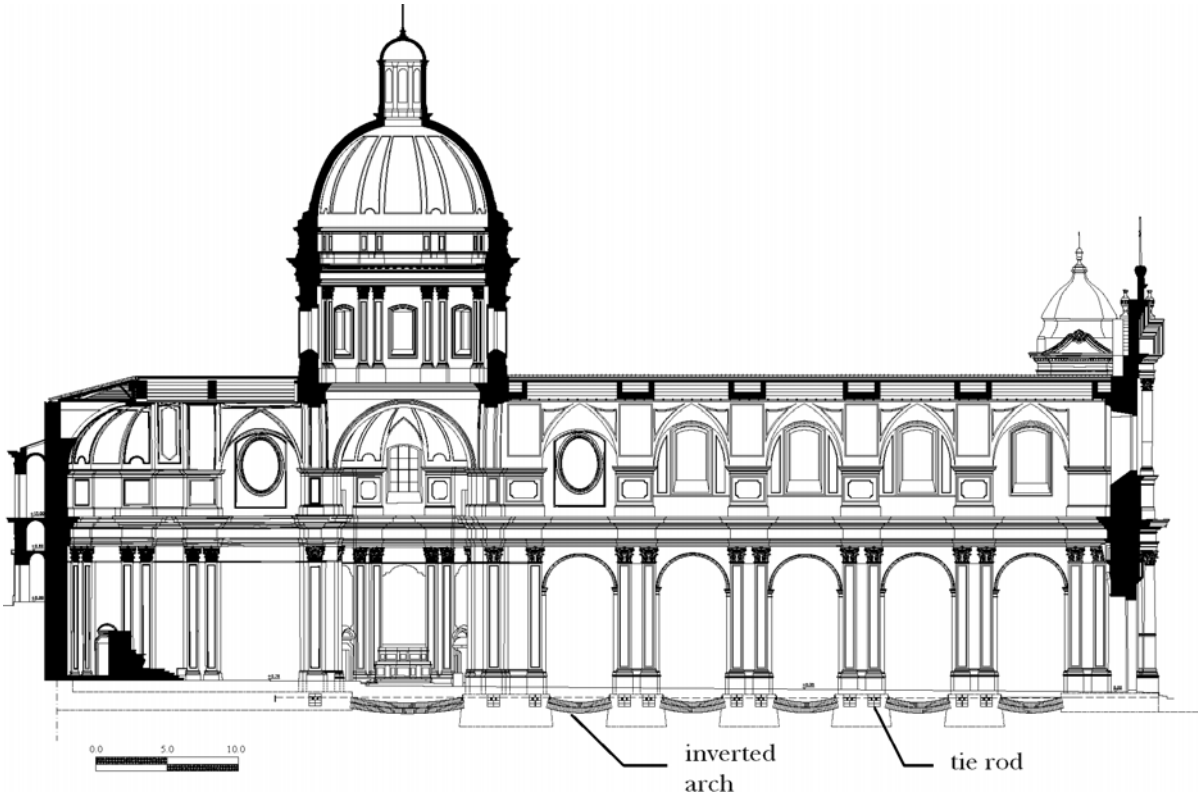

Fig. 5 – Longitudinal section of Noto Cathedral with the retrofitted foundation system.
Fig. 5 – Sezione longitudinale della Cattedrale di Noto completa del nuovo sistema di fondazioni.

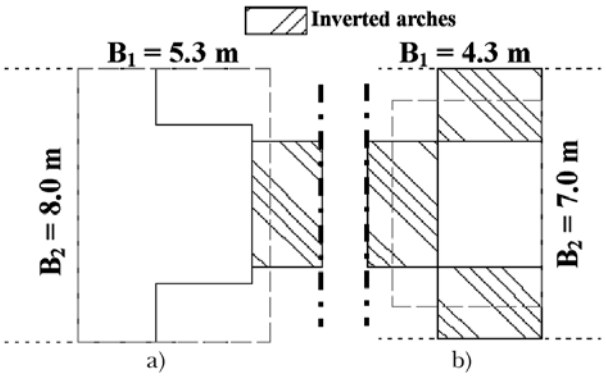

Fig. 6 – Rectangular equivalent areas of the foundations underneath the external wall (a) and the internal column (b) of the considered cross section [after MASSIMINO and MAUGERI, 2003b];
Fig. 6 – Aree rettangolari equivalenti per le fondazioni sotto il muro esterno (a) e le colonne interne (b) della sezione trasversale scelta [da MASSIMINO and MAUGERI, 2003b].

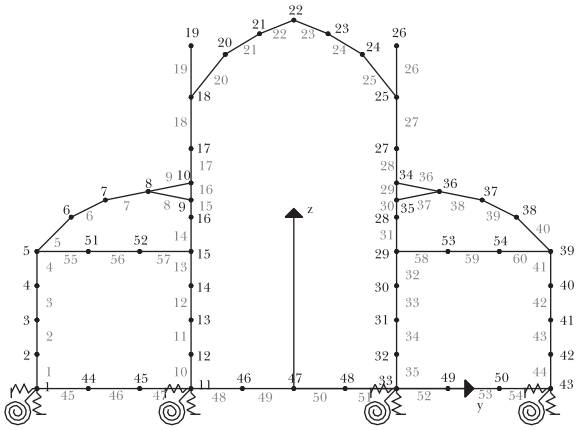

Fig. 7 – Plane structural scheme of Noto Cathedral employed for the FEM analyses, provided with tie rods.
Fig. 7 – Schema strutturale piano della Cattedrale di Noto usato per le analisi FEM, completo di barre.

iour of the masonry structure has been assumed to be linear-elastic (E_0 = 6000 MPa, ν = 0.23) [MASSIMINO and MAUGERI, 2003b]. This hypothesis is far from being realistic, since the masonry structure is damaged. However the aim of the paper is to show the effects of taking cyclic soil-structure interaction into account. The use of a more realistic non linear model for the masonry structure would obscure the effects solely due to the irreversible movements of the foundation.

3.2. Soil-structure interaction modelling

To describe the interaction between soil and structure, it is necessary to know in detail both the structure and the soil stratigraphy. The reconstruction design [TRINGALI and DE BENEDICTIS, 2000a; 2000b], which is still in progress, is based on extensive geotechnical [CAVALLARO and MAUGERI ., 2003] and structural [BINDA and MAUGERI, 1999; 2000] investigations. After the partial collapse of 1996, spe-

Tab. III – Geometrical characteristics of the masonry structural element sections [after Massimino *et al.*, 2003b].
Tab. III – Caratteristiche geometriche delle sezioni degli elementi in muratura che costituiscono la struttura [da Massimino et al.*, 2003b].*

Type of section	Area (m^2)	Moment of inertia (m^4)	Height (m)	Shear factor
1	22.00	38.250	4.568	1.672
2	20.00	10.420	2.500	0.000
3	10.00	5.210	2.500	0.000
4	2.89	0.696	1.700	0.000
5	7.29	4.430	2.700	0.000
6	15.34	15.250	3.454	1.885

cific geotechnical investigations were performed underneath the whole Noto area and in particular underneath Noto Cathedral, involving boreholes and in-situ SPT, D-H, C-H, piezometric, pressuremetric and inclinometer tests, as well as surface wave measurements. Laboratory tests were also performed, including resonant column tests, monotonic and cyclic triaxial tests and cyclic loading torsional shear tests. The main results of the geotechnical characterisation are reported in Cavallaro *et al.* [2003] and in Cavallaro and Maugeri [2003]. As regards the general characteristics and index properties of Noto Pliocene soil, which mainly consists on a medium stiff, overconsolidated lightly cemented silty-clayey-sand, it was found that the natural moisture contents w_n = 12-37 %; and the Atterberg limits are w_L = 37-69 %, w_P = 17-22 %, with a plasticity index I_P = 15-47 %. As regards the strength parameters, c' ranges between 0 kPa and 85 kPa, while ϕ' ranges between 16° and 33°. In general, the site geotechnical characterization shows a low degree of homogeneity with depth [Cavallaro and Maugeri, 2003].

In particular, the soil underneath Noto Cathedral consists mainly of: a) talus material up to a depth variable in the range of 0.5 – 5.5 m; b) highly weathered, weakly cemented, limestone, sometimes with a large clay content, up to a depth variable in the range of 12.0 – 21.5 m; c) sandy clay, which lies below the limestone and is sometimes mixed with it. Eleven SPT profiles, obtained specifically for the foundation soil of Noto Cathedral, allow the estimation of the V_s shear wave profiles according to the expressions given by Otha and Goto [1978] and Yoshida and Motonori [1988]. Thus, using the elastic relationship $G_0 = \rho\, V_s^2$, it is possible to obtain the small strain shear modulus G_0 profiles. The values of G_0 were also directly determined by means of cyclic loading torsional shear tests (CLTST) and resonant column tests (RCT) performed on some undisturbed specimens [Cavallaro *et al.*, 2003]. Good agreement was found between in-situ test results and laboratory test results [Massimino *et al.*, 2003a].

Tab. IV – Geotechnical soil characteristics [after Cavallaro *et al.*, 2003].
Tab. IV – Caratteristiche geotecniche del terreno [da Cavallaro et al.*, 2003].*

γ(kN/m^3)	G_0(MPa)	v	ϕ'(°)	c'(kPa)
19.30	92	0.30	24	15

As regards the soil-structure interaction analysis reported in the present paper, only the first soil layer of dry clayey limestone, underneath the investigated cathedral cross-section, is taken into account; according to Richard *et al.* [1993], for the analysed case the possible shallow foundation failure surface is in fact localised in this first layer. Its geotechnical characteristics are given in Table IV.

In the following two distinct interaction models will be employed: the standard elastic one characterised by three uncoupled linear springs (Fig. 4) and a coupled elasto-hypoplastic one (SFCM). The elastic response of the latter coincides with that one can be obtained by means of the former model.

The elastic stiffness coefficients depending both on the foundation geometry and soil deformability have been evaluated by following the Gazetas [1991] approach for embedded foundations:

$$K_v = K_{v,sur}\cdot\left[1+\frac{1}{21}\cdot\frac{D}{B^*}\cdot(1+1.3\chi^*)\right]\cdot\left[1+0.2\cdot\left(\frac{A_w}{A_b}\right)^{2/3}\right] \quad (10.a)$$

$$K_h = K_{h,sur}\cdot\left(1+0.15\sqrt{\frac{D}{B^*}}\right)\cdot\left[1+0.52\cdot\left(\frac{h}{B^*}\,\frac{A_w}{L^{*2}}\right)^{0.4}\right] \quad (10.b)$$

$$K_\theta = K_{\theta,sur}\cdot\left\{1+1.26\,\frac{d}{B^*}\left[1+\frac{d}{B^*}\left(\frac{d}{D}\right)^{-0.2}\sqrt{\frac{B^*}{L^*}}\right]\right\} \quad (10.c)$$

where $K_{v,sur}$, $K_{h,sur}$ and $K_{\theta,sur}$ are the vertical, horizontal and rocking stiffnesses for foundations resting on the soil surface, respectively, defined as:

$$K_{v,sur} = \frac{2\cdot G\cdot L^*}{1-v}\cdot(0.73+1.54\,\chi^{*0.75}) \quad (10d)$$

$$K_{h,sur} = \frac{2\cdot G\cdot L^*}{2-v}\cdot(2+2.50\cdot\chi^{*0.85}) \quad (10e)$$

$$K_{\theta,sur} = \frac{G}{1-v}\cdot I_{bx}^{0.75}\cdot\left(\frac{L^*}{B^*}\right)^{0.25}\cdot\left(2.4+0.5\,\frac{B^*}{L^*}\right) \quad (10f)$$

B^* and L^* are half width and half length of the rectangular foundation ($L^*>B^*$). D and d are the foundation depth and thickness, h is equal to d/2,

Tab. V – Initial values of the stiffnesses for the foundation-soil systems at nodes 1, 11, 33 and 43 of the chosen cross section (see fig.4).
Tab. V – Valori iniziali delle rigidezze per i sistemi fondazione-terreno dei nodi 1, 11, 33 e 43 della sezione trasversale scelta.

	K_h (MN/m)	K_v (MN/m)	K_θ (MNm)
Foundation of the external walls	2500	2385	22802
Foundation of the columns	2847	2373	27144

$\chi^* = A_b/4L^{*2}$, where A_b is the area of the rectangular foundation equivalent to the arbitrarily–shaped mat foundation. Furthermore A_w is the total sidewall-soil contact area, I_{bx} is the moment of inertia of the soil-foundation contact surface around the longitudinal x-axis [GAZETAS, 1991].

The values of the horizontal, vertical and rocking static stiffness coefficients employed in the numerical analyses are reported in Table V. Soil deformability, which is expressed in terms of the soil shear modulus G, is included in $K_{v,sur}$, $K_{h,sur}$ and $K_{\theta,sur}$.

As far as the elasto-hypoplastic SFCM model employed for Noto Cathedral case-history is concerned, we must add to the previously defined elastic spring stiffnesses the constitutive parameters characterising the failure locus shape (V_M, μ, ψ, β), the plastic stiffness (R_0, α, λ, χ and γ^*) and the cyclic mechanical behaviour ($\tilde{\xi}_1$ and $\tilde{\xi}_2 = \tilde{\xi}_3$). The values assigned to these different constitutive parameters are reported in Table VI.

In particular, the values of μ and ψ have been derived from Eqs. (3) and (4), with δ (interface friction angle) = 16°, while V_M was obtained from the standard bearing capacity formula of Brinch-Hansen, with c' = 15 kPa, ϕ' = 24° [CAVALLARO *et al.*, 2003], by having imposed for B_2 and D the values of MASSIMINO and MAUGERI [2003b]. R_0 has been evaluated by means of an empirical relation proposed by MONTRASIO and NOVA [1997], considering the soil as a very dense granular material. The values of β, α, $\overline{\gamma}$, λ and χ have been assumed to be the same of those previously calibrated for sandy soils. It has been proven in fact by MONTRASIO and NOVA [1997] that the exact values of these parameters have only a small influence on the calculated results. In other words these variables could be also considered as model constants. As far as the remaining constitutive parameters governing the cyclic mechanical response are concerned ($\tilde{\xi}_1$ and $\tilde{\xi}_2 = \tilde{\xi}_3$), unfortunately experimental test data for calibration are not available. As a consequence, in the present paper the values concerning dense sand homogeneous strata, calibrated by two of the authors on small scale and large scale experimental test results [DI PRISCO *et al.*, 2003] have been used. Mainly for this reason the subsequent numerical simulations must be interpreted as methodological exercises without pretending to quantitatively reproduce the actual structure response under seismic loading.

4. Numerical results of pseudo-static analyses

In this section, to simulate the seismic actions applied to the structure during an earthquake, the pseudo-static approach is followed. In the first phase, the structure is loaded by the static vertical forces corresponding to the structure weight. During the second phase, to each node of the 2-D structure of Figure 7 the pseudo-static horizontal forces related to the seismic actions are applied, so that for the i^{th} node:

$$H_i = k_h \cdot W_i \qquad (11)$$

where k_h is the seismic coefficient and W_i the weight of the sub-structure related to the i^{th} node, evaluated by means of the influence area criterion. In the present case the value of k_h is chosen to be equal to 0.22. This is the maximum value given by the site-dependent design spectrum estimated by MASSIMINO and MAUGERI [2003a], via a non linear seismic response analysis of the foundation subsoil and, thus, through the comparison between the computed average design spectrum and the EC8 design spectrum [MASSIMINO and MAUGERI, 2003a] (see Fig. 8). In particular, the maximum value of the proposed site-dependent design spectrum represents the average value of the spectral accelerations in the range of periods T = 0.10. 10–0.75 sec.

Tab. VI – Constitutive parameters of the elasto-hypoplastic SFCM model for Noto Cathedral.
Tab. VI – Parametri costitutivi del modello elastico-ipoplastico SFCM utilizzato per la cattedrale di Noto.

Foundation characteristics			Parameters of the modified sfcm model										
Node	B_2 (m)	D (m)	β	α	γ^*	μ	ψ	λ	χ	$\tilde{\xi}_1$	$\tilde{\xi}_1 = \tilde{\xi}_3$	R_0 (kN/m)	V_M (kN)
1 and 43	8.00	1.25	0.95	2.83	1.71	0.40	0.40	0.80	0.286	4	20	86349	25585
11 and 33	7.00	2.50	0.95	2.83	1.71	0.54	0.46	0.80	0.286	4	20	100393	26028

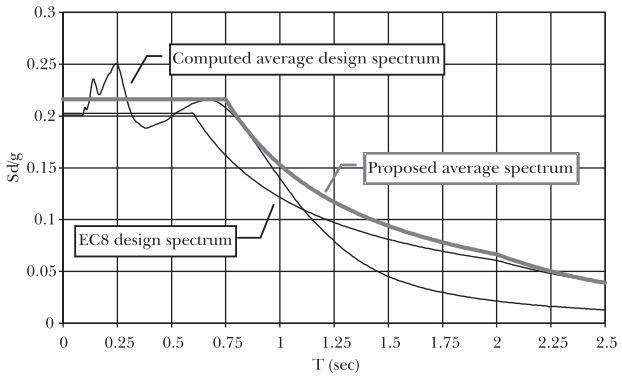

Fig. 8 – Comparison between the computed average design spectrum, the EC8 spectrum and the proposed one [after MASSIMINO and MAUGERI, 2003a].
Fig. 8 – Confronto fra lo spettro di progetto medio calcolato, lo spettro suggerito dal EC8 e quello proposto da MASSIMINO and MAUGERI, [2003a].

4.1. Pseudo-static linear-elastic numerical analysis

The hypothesis of linear-elastic soil behaviour is not realistic, but because of its simplicity, it is largely employed in routine design. To validate the elastic part of the hypoplastic code, the results obtained by disregarding the plastic components were firstly successfully compared with those published by MASSIMINO and MAUGERI [2003b]. The effect of tie rods was subsequently investigated. The vertical as well as the horizontal forces and the overturning moments transferred to the foundations are similar in the two cases (Fig. 9a), and the generalised displacements approximately coincide (Fig. 9b). According to the elastic analysis simulations, it seems that tie rods have no practical influence on the mechanical response of the foundation. This, clearly unrealistic, conclusion will be contradicted by the elastoplastic analysis discussed in the following.

The maximum horizontal and vertical displacement values are recorded at node 43 for both schemes, including and not including tie rods. Moreover, focusing our attention to the scheme including tie rods, the maximum horizontal differential displacement, which is reached between nodes 33 and 43, is equal to 0.54 mm. The maximum vertical differential displacement, reached between nodes 33 and 43, is equal to 1.23 mm. With reference to the superstructure, the maximum horizontal displacement, equal to 6.05 mm, is reached at node 26 (Fig. 10), i.e. at the right side of the central arch, while the maximum vertical displacement, equal to 4.16 mm, is reached at node 20 (Fig. 10), i.e. at the left side of the central arch.

The deformed configuration of the employed plane scheme considering the pseudo-static forces, the presence of tie rods is shown in Figure 10. The displacements of all the nodes are amplified by a factor equal to 100 for a better visual representation of the deformed configuration.

4.2. Pseudo-static elasto-hypoplastic numerical analyses

In this paragraph, the numerical results obtained by means of the elasto-hypoplastic SFCM soil model are discussed. It is worth noting that when only monotonic loading is considered, the SFCM elasto-hypoplastic model coincides with the NOVA-MONTRASIO [1991] model, because the image point of the generalised states of stress always belong to the yield surface. The values of H, V and M transferred from the superstructure to the foundation

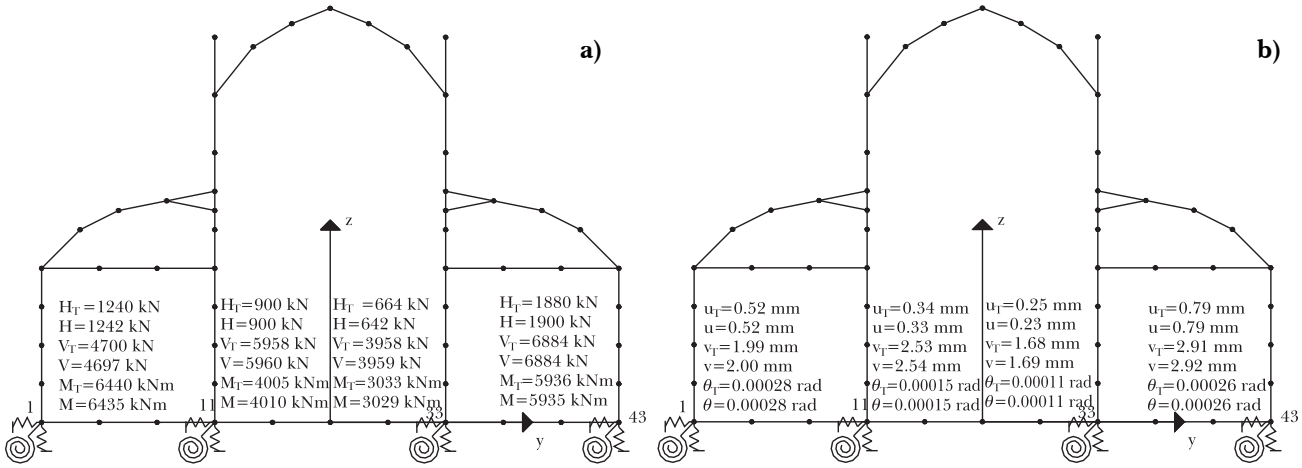

Fig. 9 – Comparison of the calculated values with (index T) and without tie-rods (no index), considering a linear-elastic soil behaviour for the nodes 1, 11, 33 and 43 of a) H, V and M transferred from the superstructure to the foundations, b) horizontal (u) and vertical (v) displacements and rotations (θ).
Fig. 9 – Confronto dei valori per i nodi 1, 11, 33 e 43 calcolati in presenza (indice T) ed in assenza dei tiranti (nessun indice), considerando un comportamento elastico-lineare del terreno: a) Forze e momenti ribaltanti trasferiti dalla sovrastruttura alla fondazioni, b) spostamenti orizzontali (u,) verticali (v) e rotazioni (θ).

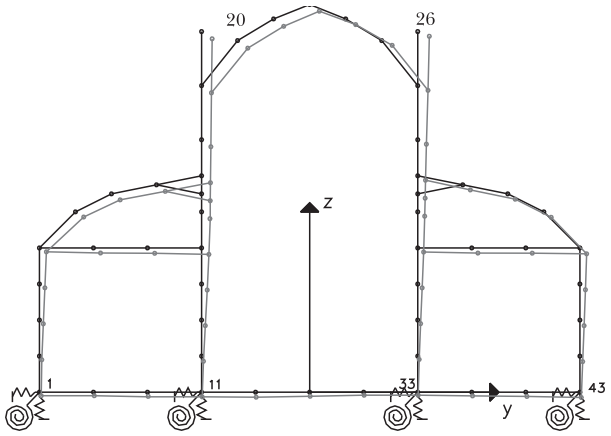

Fig. 10 – Deformed configuration of the structure, considering tie rods and a linear-elastic soil behaviour.
Fig. 10 – Deformata strutturale, considerando le barre ed un comportamento elastico-lineare del terreno.

obtained considering (index T) and not considering (no index) tie rods are reported in Figure 11. For both analyses, the maximum values of H are reached at node 11 and not at node 43 (as in the elastic case), the maximum values of M are reached at node 11 and not at node 1 as in the elastic case, while the maximum value of V is reached at node 43, analogously to the elastic case previously considered.

In this case, the presence of tie-rods can be appreciated. They marginally influence the horizontal and vertical force values transferred from the superstructure to the foundation, while the overturning moment changes for all the foundation nodes accordingly to the tie-rod presence. By comparing Figure 9 and Figure 11 (index T), it is worth noting that the vertical forces are quite similar considering either the linear-elastic soil behaviour or an elasto-hypoplastic soil response (a maximum difference of 7% is obtained), while both horizontal forces (about 48%) and overturning moments (about 60%) severely differ. Finally, horizontal and vertical displacement and rotation values for the foundation nodes 1, 11, 33 and 43, with and without tie rods, are reported in Figure 12.

The presence of the tie-rods induces larger horizontal absolute displacements at nodes 1 and 11, whereas it is true the opposite for nodes 33 and 43. In particular, if we take into consideration the central nodes 11 and 33, it is evident that the horizontal differential displacement decrease severely. Moreover, the vertical absolute displacements are smaller when tie rods are considered. Including tie rods, smaller vertical differential displacements can be observed between nodes 1-11 and 11-33, while a larger vertical differential displacement occurs between nodes 33 and 43.

As regards the whole structure, when tie-rods are present, the maximum horizontal displacement, equal to 36.8 mm, is reached at node 26, while the maximum vertical displacement, equal to 40.8 mm, is reached at node 20. When the tie-rods are absent, the maximum horizontal displacement, equal to 38.3 mm, is reached at node 26, while the maximum vertical displacement, equal to 46.3 mm, is reached at node 21.

The deformed configuration of the used plane structural scheme, considering the pseudo-static approach, the presence of tie-rods and the elasto-hypoplastic SFCM soil model, is shown in Figure 13.

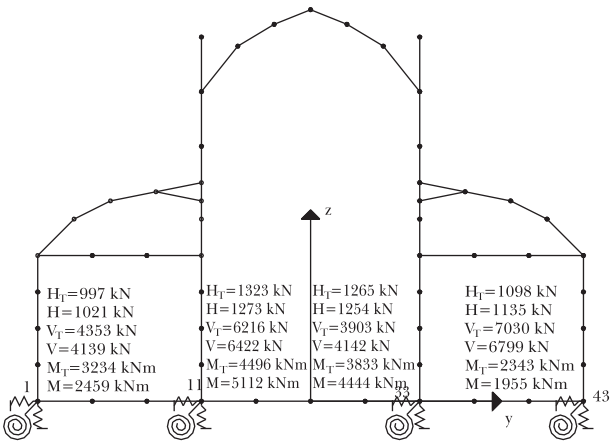

Fig. 11 – Comparison of the values of H, V and M transferred from the superstructure to the foundations obtained with (index T) and without tie-rods (no index), considering the elasto-hypoplastic SFCM soil model.
Fig. 11 – Confronto dei valori di H, V e M trasferiti dalla sovrastruttura alle fondazioni ottenuti in presenza (indice T) e in assenza dei tiranti (nessun indice), considerando il modello elastico-ipoplastico SFCM per il terreno.

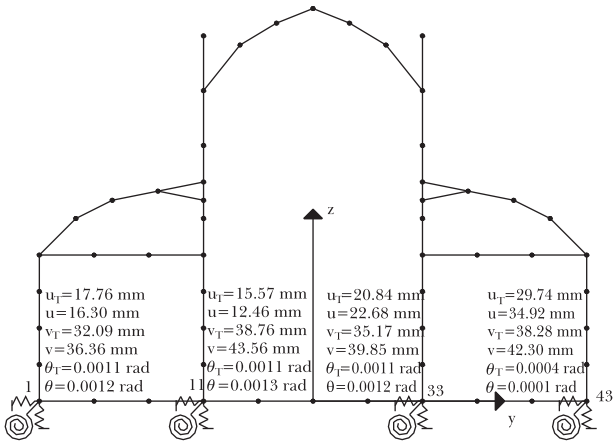

Fig. 12 – Comparison of the horizontal (u) and vertical (v) displacements and rotations (θ) for the nodes 1, 11, 33 and 43 obtained with (index T) and without tie-rods (no index), considering the elasto-hypoplastic SFCM soil model.
Fig. 12 – Confronto degli spostamenti orizzontali (u) e verticali (v) e delle rotazioni (θ) per i nodi 1, 11, 33 e 43 ottenuti in presenza (indice T) e in assenza dei tiranti (nessun indice), considerando il modello elasto-ipoplastico SFCM per il terreno.

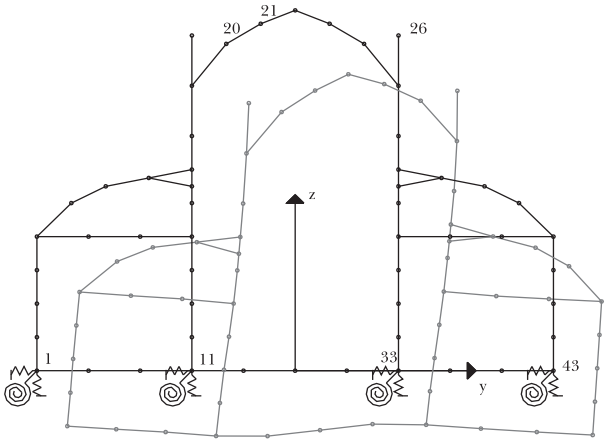

Fig. 13 – Deformed configuration of the structure, considering tie rods and the elasto-hypoplastic SFCM soil model.
Fig. 13 – Deformata strutturale,considerando le barre e il modello elastico-ipoplastico SFCM per il terreno.

Tab. VII – Values of H, V and M transferred from the superstructure to the foundations, considering the seismic coefficient k_h*.
Tab. VII – Valori di H, V e M trasferiti dalla sovrastruttura alle fondazioni, considerando il coefficiente sismico k_h.*

Node	H (kN)	V (kN)	M (kNm)
1	722	4745	2350
11	675	5907	2521
33	844	4625	3168
43	569	6225	1526

The displacements of all the nodes are amplified by a factor equal to 100 for a better representation of the deformed configuration. From Figure 13, we derive that the structural response of the Cathedral is dominated by the stiffness of the two lateral naves because the constraint given by the central nave is negligible. This means that the two lateral sub-structures behave approximately as independent bodies [MASSIMINO *et al.*, 2004].

The analysis performed in this section, taking into account the tie-rod presence shows that the arch of the central nave is subjected to large horizontal displacements and as a consequence it should be considered as the most vulnerable element of the whole structure. This element, in fact, will be reinforced by carbon fibers.

To analyse the behaviour of Noto Cathedral under a moderate and more frequent earthquake scenario, an additional numerical analysis has been performed by applying the 60% of the seismic coefficient k_h of Eq.(11) in the following named k_h*. In Table VII the relative values of H, V and M transferred by the superstructure to the foundation are reported.

Tab. VIII – Horizontal (u) and vertical (v) displacements and rotations (θ) for the nodes 1, 11, 33 and 43, considering the seismic coefficient k_h*.
Tab. VIII – Spostamenti orizzontali (u) e verticali (v) e rotazioni (θ) per i nodi 1, 11, 33 e 43, considerando il coefficiente sismico k_h.*

Node	u (mm)	v (mm)	θ (rad)
1	3.73	22.93	0.0007
11	4.62	25.88	0.0005
33	7.91	23.58	0.0004
43	14.29	25.15	0.0002

If we consider H and M, we can observe that the maximum values, when the seismic coefficient is k_h*, are reached at node 33, while when the seismic coefficient is k_h at node 11 (Fig. 11).

On the contrary, the maximum value of V is reached in both cases at node 43. The values of the horizontal and vertical displacements and rotations for the foundation nodes 1, 11, 33 and 43 are reported in Table VIII.

5. Numerical results for cyclic loading analyses

When seismic soil-structure interaction problems are studied, the pseudo-static approach represents the most simple way. Nevertheless, it can often lead to erroneous results because two factors are disregarded: the cyclic change of loading distribution within the structure during the seismic event and the importance of the loading frequency on the dynamic response of the structure.

In this paper, only the former factor is taken into consideration and, as a consequence, FEM cyclic quasi-static analyses have been performed. In this case, the soil-foundation interaction is assumed to be described uniquely by the elasto-hypoplastic SFCM model described previously. The 2-D structure of Figure 7 has been loaded by 40 H cycles whose amplitude is evaluated by means of the k^*_h coefficient defined in the previous paragraph.

Many different horizontal cyclic force amplitudes at increasing k_h coefficient have been taken into consideration. For instance, we obtain, for n = 40, the failure of the footing corresponding to the node 1, for a loading amplitude equal to 65 % of the k_h value applied in the pseudo-static tests (k_h = 0.143). For this case, in Figure 14, the evolution of variables H, V and M at nodes 1 and 11 of Figure 7 are illustrated.

The loading paths relative to the pseudo-static analyses are superimposed and, in the first phase, the two loading paths coincide.

It is evident the decrease with time in the V value for the foundation node 1, while if we consider

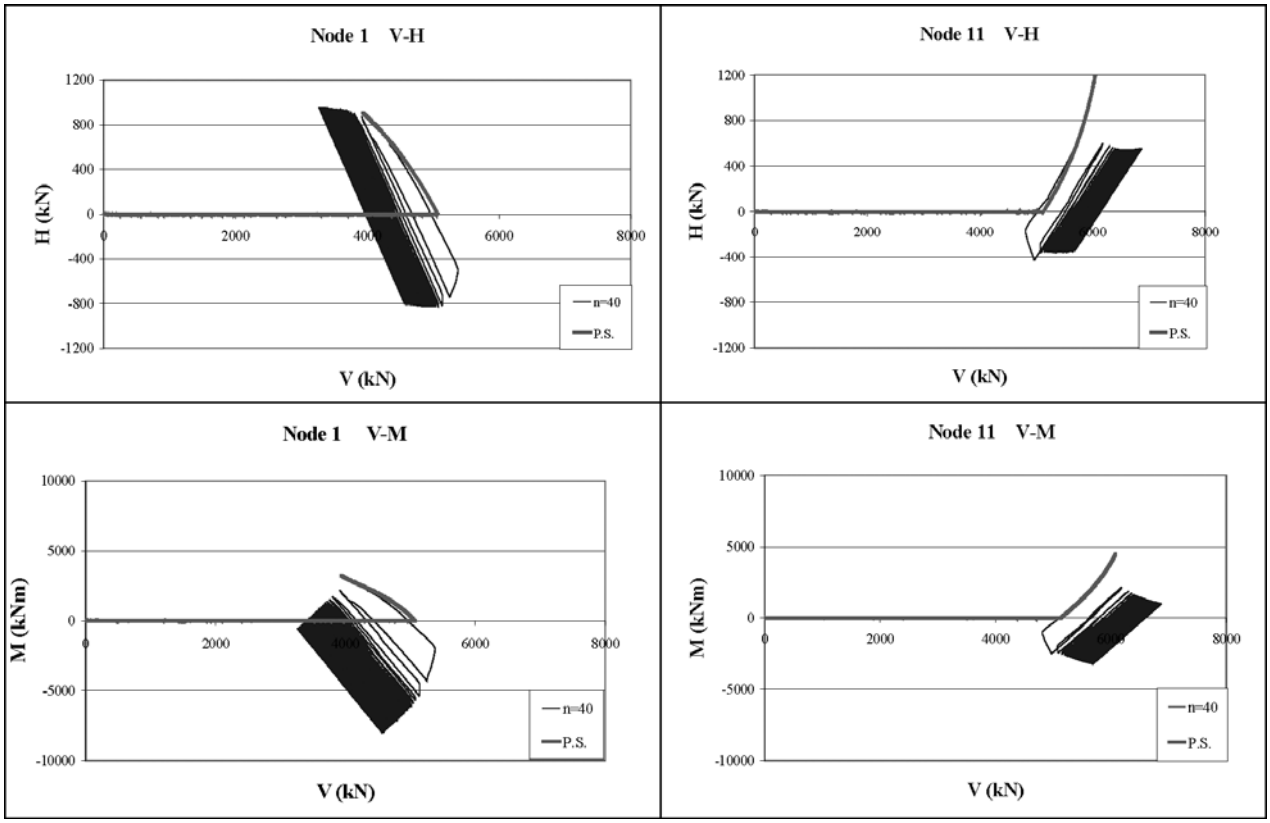

Fig. 14 – Curves V versus H and V versus M for the foundation nodes 1 and 11 for monotonic and cyclic loading (k_h=0.143).
Fig. 14 – Curve V-H e V-M per i nodi di fondazione 1 e 11 per carico ciclico e monotono (k_h=0.143).

node 11, we observe the opposite trend. If we compare the generalised stress paths with the corresponding failure loci both in the H-V and M-V planes (Figs. 15 and 16), we can easily conclude that the most dangerous generalised stress path occurs at node 1. In fact, by decreasing the V value, the image point approaches the failure locus in the sliding branch.

The coupling of the generalised stresses causes a simultaneous degradation of the constraints and renders ill-constrained an original over conditioned structure (the left nave substructure). The failure of the foundation at node 1 implies therefore the collapse of the entire left side nave.

It is worth noting that if we impose a cyclic loading characterised by an amplitude equal to the 80 % of the k_h value applied in the pseudo-static analyses, the number of cycles corresponding to failure is equal to 0.75: i.e. during the first cycle and, in particular, when the horizontal forces reach the maximum negative value, collapse of the right footing (node 43) takes place. On the contrary, if we decrease the cyclic amplitude under 40 %, the number of cycles to be applied to reach failure rapidly increases and the system becomes stable even in cyclic conditions.

In Figures 17 and 18, the horizontal and vertical displacements of the footing nodes 1, 11, 33 and 43 are shown, while the values of these displacements, as well as the values of the rotations of the footing nodes 1, 11, 33 and 43, are reported in Table IX.

Tab. IX – Horizontal (u) and vertical (v) displacements and rotations (θ) for nodes 1, 11, 33 and 43 for cyclic loading, considering the presence of tie-rods.
Tab. IX – Spostamenti orizzontali (u) e verticali (v) e rotazioni (θ) per i nodi 1, 11, 33 e 43 per carico ciclico, considerando la presenza dei tiranti.

Node	u (mm)	v (mm)	θ (rad)
1	7.13	37.20	0.00032
11	4.64	30.01	0.00016
33	4.70	27.90	0.00009
43	5.62	31.16	0.00004

The deformed configuration of the structural scheme, in the cyclic approach, with tie-rods and the hypo-plastic SFCM soil model, is shown in Figure 19.

The profile of the deformed foundation is more or less independent of the number of cycles (after the first virgin loading and before collapse) and symmetric with respect to the axis of symmetry of the Cathedral. By comparing Figures 19 and 13 we can note that the pseudo-static analysis gives instead an anti-symmetric profile.

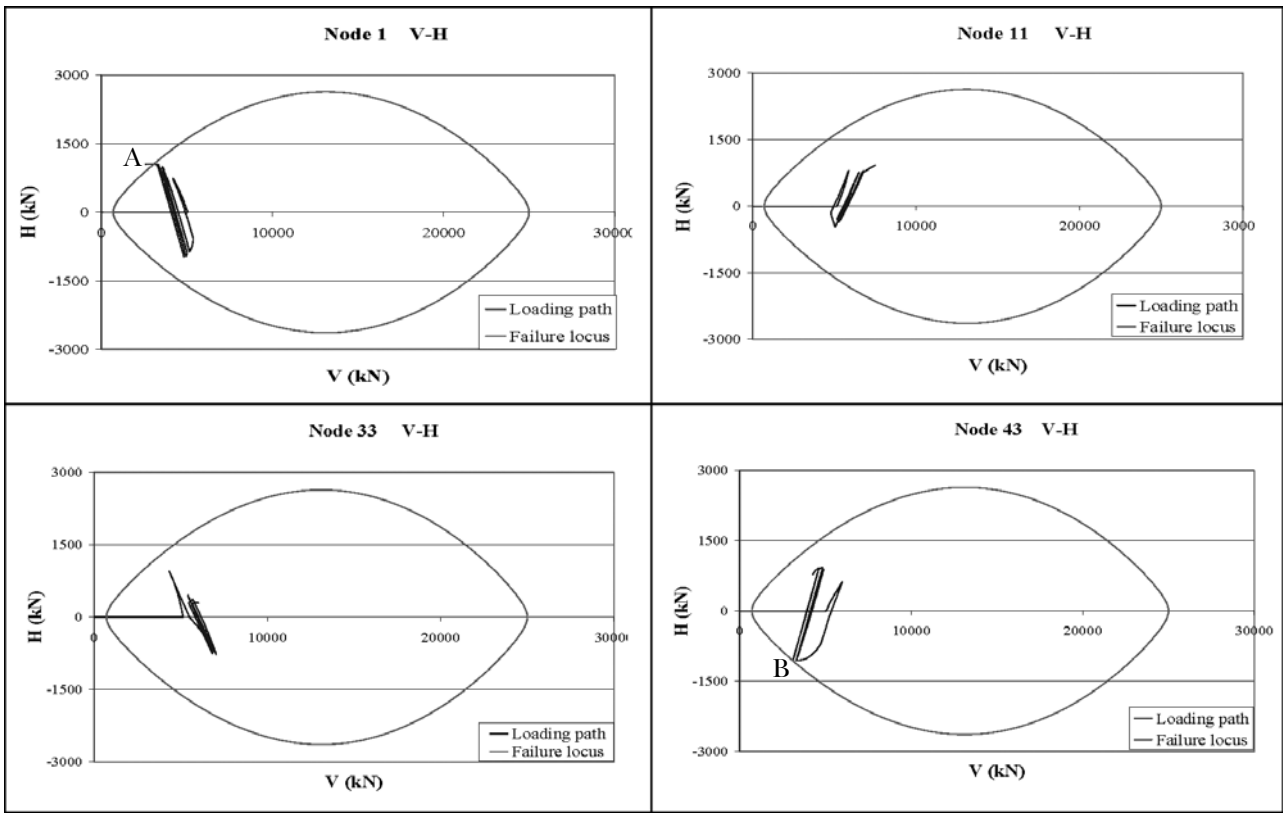

Fig. 15 – V-H loading paths for nodes 1, 11, 33 and 43 and corresponding failure loci.
Fig. 15 – Percorsi di carico generalizzati V-H dei nodi 1, 11, 33 e 43 e corrispondenti luoghi di rottura.

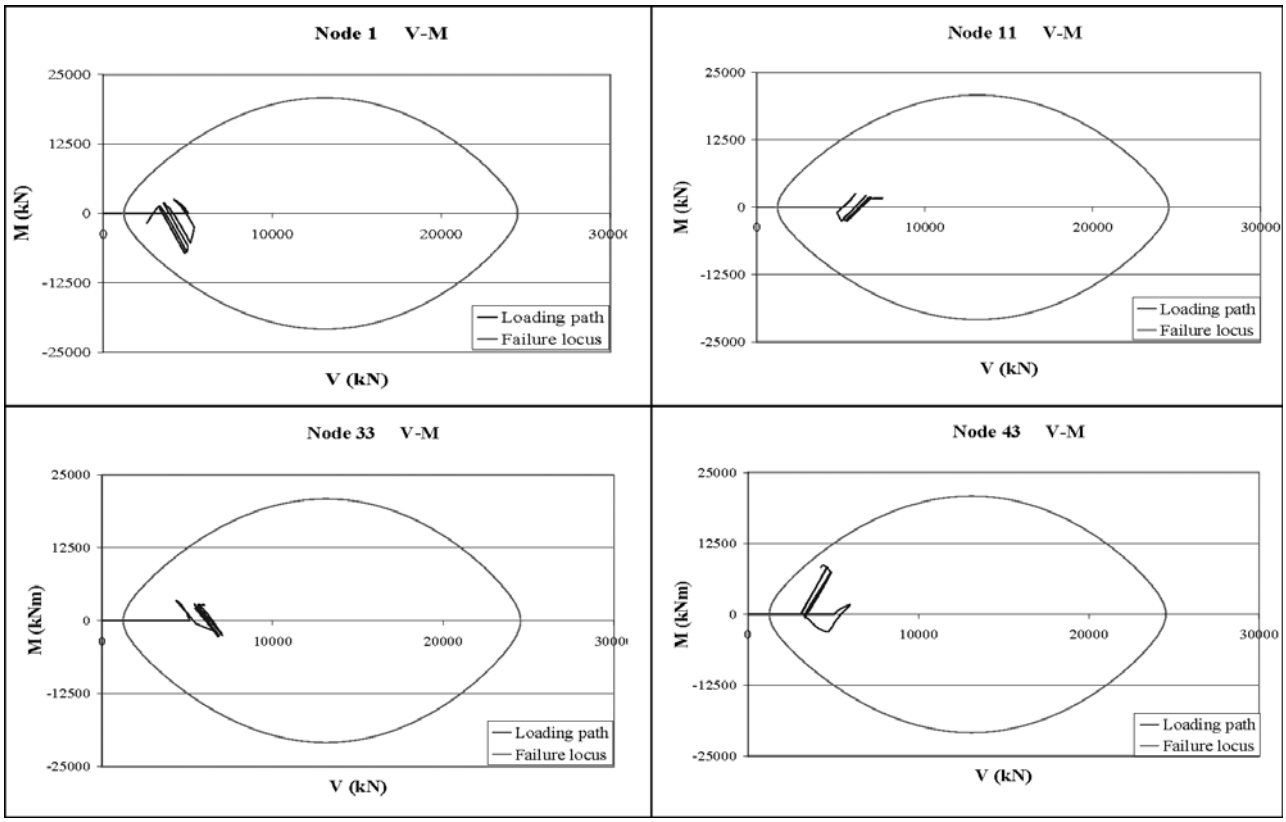

Fig. 16 – V-M loading paths for nodes 1, 11, 33 and 43 and corresponding failure loci.
Fig. 16 – Percorsi di carico generalizzati V-M dei nodi 1, 11, 33 e 43 e corrispondenti luoghi di rottura.

To compare the horizontal and vertical displacements obtained by means of all the FEM analyses performed, in Tables X and XI some summarising data are reported. The maximum horizontal displacements are reached at the nodes of the nave arch. The horizontal displacements obtained by means of the pseudo-static approach are larger than those obtained by means of the cyclic approach. This is due to the fact that in cyclic conditions horizontal forces do not increase monotonically but change sign continuously. The asymmetric mechanical response of the foundation elements is at any rate due to the initial asymmetry of the horizontal actions: this means that the initial sign of the seismic action influence irreversibly the successive structural response.

On the contrary (Tab. XI), it is evident that (see also Fig. 14) the vertical displacements of three foundation nodes (11, 33 and 43) decrease by taking into consideration the cyclic loading, while at node 1, where the collapse takes place (Fig.15), the vertical displacement increases.

6. Concluding remarks

The building seismic retrofitting of monuments and ancient is of great importance particularly in an area as Eastern Sicily subjected to a high seismic hazard.

After the damage consequent to "Santa Lucia" earthquake of December 13th 1990, the Noto Cathedral suffered in 1996 a partial but catastrophic collapse. As a consequence, in the recent past, the Cathedral has been widely studied, both from a structural and a geotechnical viewpoint.

The Cathedral has been numerically discretised by means of beam elements, the footings have been assumed to be rigid, whereas the soil-structure interaction has been simulated by following the "macro-element" concept. The attention has been concentrated on the footing mechanical response and, for this reason, the structure has been assumed to be elastic whereas the soil-foundation system has been simulated both by an elastic and an elasto-hypoplastic constitutive relationships.

Tab. X – Horizontal displacements obtained by the different FEM analyses performed.
Tab. X – Spostamenti orizzontali ottenuti dalle differenti analisi FEM eseguite.

Node	u (mm)			
	L.E._P.S.	E.H.P._P.S.	E.H.P._P.S. (60%)	E.H.P._C.
1	0.52	17.76	3.73	7.13
11	0.34	15.57	4.62	4.64
33	0.25	20.84	7.91	4.70
43	0.79	29.74	14.29	5.62

L.E._P.S. = pseudo-static analysis, considering a linear-elastic soil behaviour.
E.H.P._P.S. = pseudo-static analysis considering the elasto-hypoplastic SFCM soil model.
E.H.P._P.S. (60%) = pseudo-static analysis considering the elasto-hypoplastic SFCM soil model and k_h*.
E.H.P._C. = cyclic analysis considering the elasto-hypoplastic SFCM soil model.

Tab. XI – Vertical displacements obtained by the different FEM analyses performed, excluding the vertical displacements due to the structure weight.
Tab. XI – Spostamenti verticali ottenuti dalle differenti analisi FEM eseguite, depurati dai cedimenti indotti dal peso proprio della struttura.

Node	v (mm)			
	L.E._P.S.	E.H.P._P.S.	E.H.P._P.S. (60%)	E.H.P._C.
1	1.99	32.09	22.93	37.20
11	2.53	38.76	25.88	30.01
33	1.68	35.17	23.58	27.90
43	2.91	38.28	25.15	31.16

L.E._P.S. = pseudo-static analysis, considering a linear-elastic soil behaviour.
E.H.P._P.S. = pseudo-static analysis considering the elasto-hypoplastic SFCM soil model.
E.H.P._P.S. (60%) = pseudo-static analysis considering the elasto-hypoplastic SFCM soil model and k_h*.
E.H.P._C. = cyclic analysis considering the elasto-hypoplastic SFCM soil model.

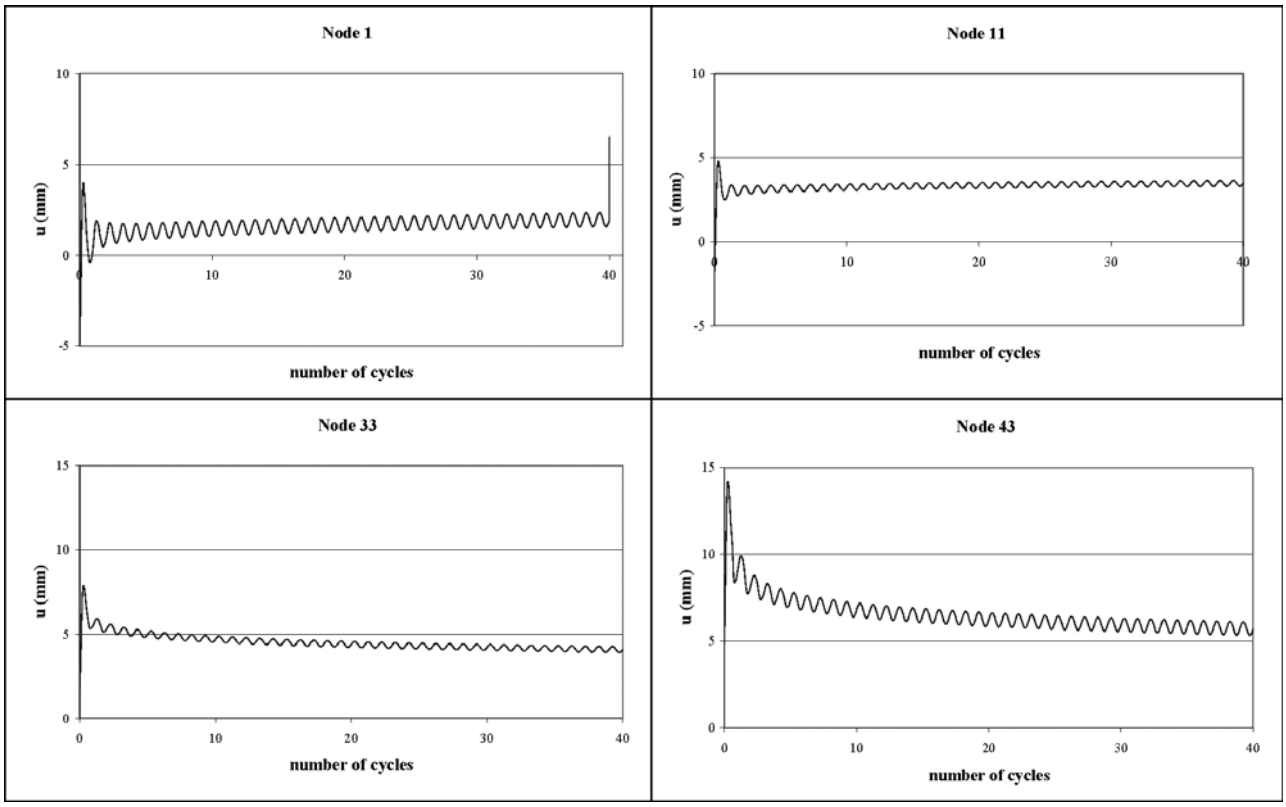

Fig. 17 – Horizontal displacements for foundation nodes 1, 11, 33 and 43 for cyclic loading.
Fig. 17 – Spostamenti orizzontali per i nodi di fondazione 1, 11, 33 e 43 per carico ciclico.

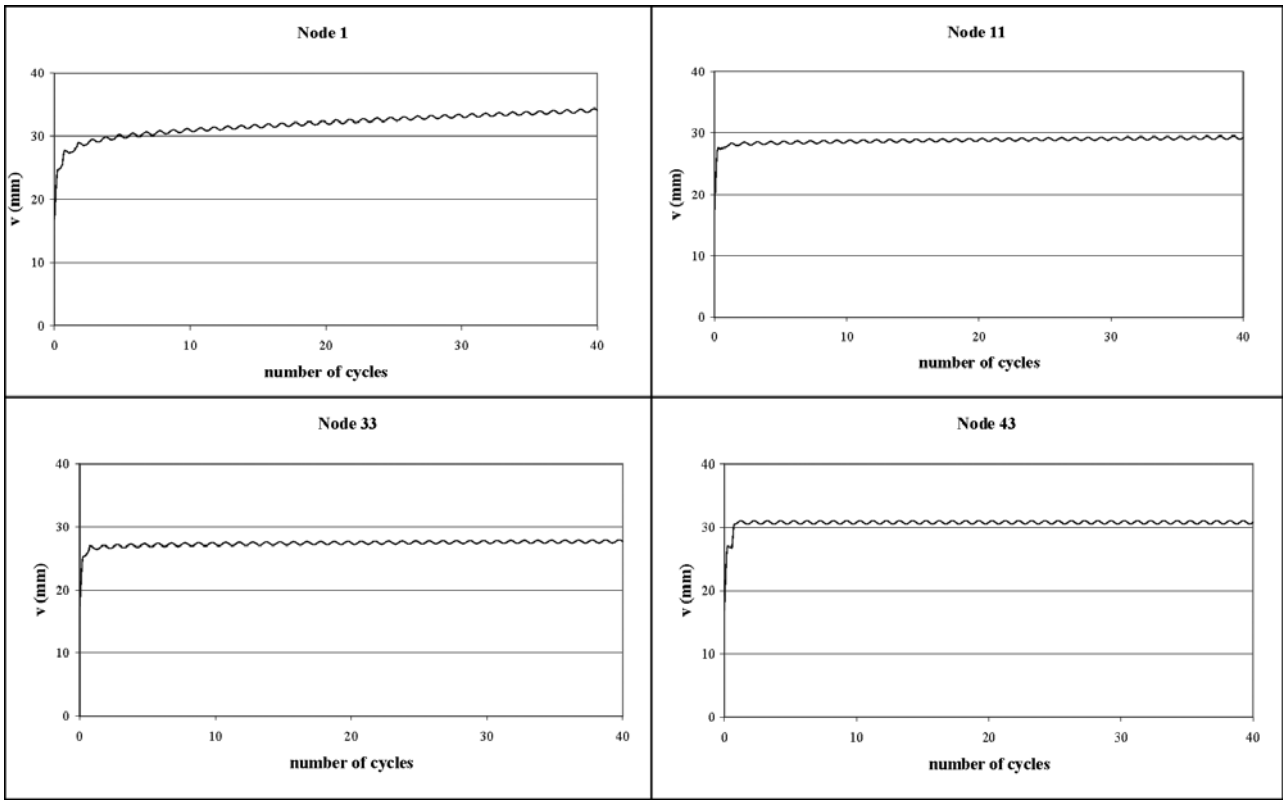

Fig. 18 – Vertical displacements for foundation nodes 1, 11, 33 and 43 for cyclic loading.
Fig. 18 – Spostamenti verticali per i nodi 1, 11, 33 e 43 per carico ciclico.

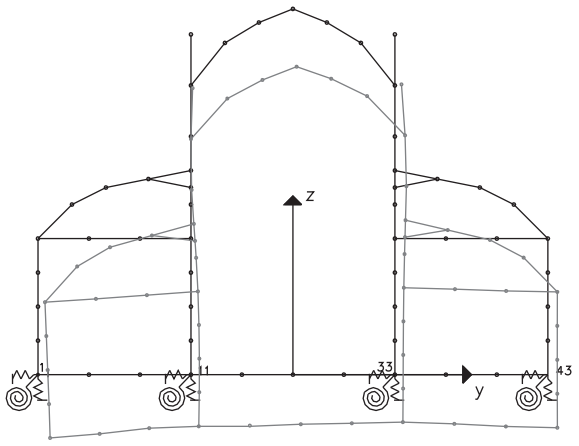

Fig. 19 – Deformed configuration of the structure in cyclic conditions, considering tie rods and the elasto-hypoplastic SFCM soil model.
Fig. 19 – Deformata strutturale in condizioni cicliche, considerando le barre e il modello elastico-ipoplastico SFCM per il terreno.

In the FEM analyses different types of soil behaviour have been considered and the comparison between the pseudo-static approach and the cyclic approach has been discussed. It has been shown in particular that the beneficial effect of tie rods connecting footings to each other can be captured only if the plastic soil behaviour is modelled. Furthermore since the structure is statically indeterminate and the constitutive relationship describing the soil-structure interaction has been assumed to be irreversible and path-dependent, the actions applied to the footings have been shown to dramatically depend on the number of cycles imposed. In particular, contrary to what one could expect, the failure can occur in cyclic conditions for loading amplitudes defined as acceptable if pseudo-static conditions are taken into consideration. For the left footing of the left nave in fact, the accumulation in vertical displacements induces a continuous decrease in the vertical load and, as a consequence, a continuous approaching to the failure locus.

Of course, the study reported in the present paper must be interpreted only as a methodological example capable of showing that, in statically indeterminate structures, cyclic irreversible displacements, analogously to what can occur for cyclic damage within the superstructure, may cause very dangerous loading redistribution on the foundations. On the other hand, it should be noted that, qualitatively, similar results could be obtained by performing FEM numerical analyses which consider the soil as a deformable continuum, if and only if this latter is described by means of a very sophisticated constitutive model capable of accumulating irreversible strains even within the yield locus. This latter type of analysis is therefore much more complex and time consuming than the simplified one here presented.

The main advantage of the macroelement concept appears anyway to be the possibility of grasping the overall structural behaviour, even in a relatively complex problem like this, with simple considerations based on the analysis of the generalised foundation stress path.

Acknowledgement

The research was financially supported by the "Fondazione Bonino-Pulejo" of Messina and by the Italian Ministry of University and Scientific Research.

References

BINDA L., BARONIO G., GAVARINI C., DE BENEDICTIS R., TRINGALI S. (1999) – *Investigation on materials and structures for the reconstruction of the partially collapsed Cathedral of Noto (Sicily)*. Proc. 6th Int. Conf. Structural Studies, Repairs and Maintenance of Historical Buildings, STREMAH 99, Dresden, Germany, pp. 323-332.

BINDA L., SAISI A., TIRABOSCHI C., VALLE S., COLLA C., FORDE M. (2000) – *Indagini soniche e radar sui pilastri e sulle murature della Cattedrale di Noto*. Proc. Int. Workshop on: "Ricostruendo la Cattedrale di Noto e la Frauenkirche di Dresda", Noto (Siracusa), Italy, pp. 91-106.

BOTTARI A., SARAÒ A., TERAMO A., TERMINI D. AND CARVENI P. (2003) – *The earthquake on January 11th 1693 in South-Eastern Sicily: macroseismic analysis and strong motion modelling in Noto*. In "Geotechnical analysis of seismic vulnerability of monuments and historical sites", Maugeri M. & Nova R. (Eds.), Pàtron, Bologna, pp. 211-222.

BUTTERFIELD R., GOTTARDI G. (1993). *A complete three-dimensional failure envelope for shallow footings on sand*, Géotechnique 44, n. 1, pp. 181-184.

BUTTERFIELD R., TICOF G. (1979) – *Discussion: Design parameters for granular soils*. Proc., 7th European Conf. on Soil Mech. Fndn. Engng., Brighton, 4, pp. 259-262.

CAMPOCCIA I., MASSIMINO M.R. (2003) – *Grade-3 seismic microzonation at Noto by synthetic input accelerograms*. In "Geotechnical analysis of seismic vulnerability of monuments and historical sites". Maugeri M. & Nova R., Pàtron, Bologna, pp. 257-286.

CAVALLARO A., MASSIMINO M.R., MAUGERI M. (2003) – *Noto Cathedral: soil and foundation investigation*. Construction and Building Materials Journal, Elsevier, 17(2003), pp. 533-541.

Cavallaro A., Maugeri M. (2003) – *Site characterization by in-situ and laboratory tests for the microzonation of Noto*. In "Geotechnical analysis of seismic vulnerability of monuments and historical sites", Maugeri M. & Nova R. (Eds.), Pàtron, Bologna, pp. 237-256.

di Prisco C., Fornari B., Nova R., Pedretti S. (1998) – *A constitutive model for cyclically loaded shallow foundations*. Proc. Of Euromech 385 Colloquium on Inelastic Analysis Structures under Variable Loads: Theory and Engineering Applications Aachen, 8-11, September 1998.

di Prisco C., Nova R., Sibilia A. (2003) – *Shallow footing under cyclic loading: experimental behaviour and constitutive modelling*. In "Geotechnical analysis of the seismic vulnerability of historical monuments", Maugeri M. & Nova R. (Eds.), Pàtron, Bologna, pp. 99-122.

Gazetas, G. (1991) – *Foundation Vibrations*. in Foundation Engineering Handbook, (H.Y. Fang, Ed.) Van Nostrand Reinhold, New York, pp. 553-593.

Massimino M.R., Maugeri M. (2003a) – *Design spectrum by synthetic accelerograms for Noto Cathedral (Siracusa, Italy)*. In "Geotechnical analysis of seismic vulnerability of monuments and historical sites", Maugeri M. & Nova R. (Eds.), Pàtron, Bologna, pp. 287-308.

Massimino M.R., Maugeri M. (2003b) – *Retrofitting of the foundation of Noto Cathedral (Italy) according to Eurocodes*. In "Geotechnical analysis of seismic vulnerability of monuments and historical sites", Maugeri M. & Nova R. (Eds.), Pàtron, Bologna, pp. 309-330.

Massimino M.R., Maugeri M., Perretti P. (2004) – *Analisi non lineare dell'interazione terreno-fondazione-sovrastruttura per la Cattedrale di San Nicolò a Noto*. Atti XXII Convegno Nazionale di Geotecnica "Sicurezza ed adeguamento delle opere esistenti", Palermo 22-24 settembre 2004, pp. 395-402.

Montrasio L., Nova R. (1988) – *Assestamenti di una fondazione modello sotto carico inclinato: risultati sperimentali e modellazione matematica*. Rivista Italiana di Geotecnica, 22, n. 1, pp. 35-49

Montrasio L., Nova R. (1997) – *Settlements of shallow foundations on sand: geometrical effects*. Géotechnique 47, n. 1, pp. 49-60.

Mylonakis G., Gazetas G. (2000) – *Seismic soil-structure interaction: beneficial or detrimental?* Journ. of Earthquake Engineering, 4(3), pp. 277-301.

Nova R., Montrasio L. (1991) – *Settlements of shallow foundations on sand*. Géotechnique, 41, n. 2, pp. 243-256.

Otha Y. and Goto N. (1978) – *Empirical shear wave velocity equations in terms of characteristic soil indexes*. Earthquake Engineering and Structural Dynamics, vol. VI.

Poulos H.G. (1975) – *Settlement analysis of structural foundation systems*. Proc. 4th SouthEast Asian Conf. on Soil Engineering Kuala Lumpur, Malaysia, 4, pp. 54-61.

Prakash S. (2004) – *Evaluation of soil-structure interaction effects of embedded structure by simple method*. Proc. 13th WCEE, Vancouver, B.C., Canada, August 1-6, 2004, paper n. 3405.

Richard R., Elms D.G., Budhu M. (1993) – *Seismic bearing capacity and settlements foundations*. Journal of Geotechnical and Engineering, 119(4), pp. 662-674.

Tringali S., De Benedictis R. (2000a) – *Il progetto di ricostruzione della Cattedrale di Noto: il sistema delle crociere e gli aspetti di impatto socio-economico sulla città e il comprensorio*. Proc. Int. Workshop on: "Ricostruendo la Cattedrale di Noto e la Frauenkirche di Dresda", Noto (Siracusa), Italy, pp. 143-149.

Tringali S., De Benedictis R. (2000b) – *Il progetto di ricostruzione della Cattedrale di Noto: il sistema delle navate*. Proc. Int. Workshop on: "Ricostruendo la Cattedrale di Noto e la Frauenkirche di Dresda", Noto (Siracusa), Italy, pp. 151-158.

Yoshida Y., Motonori I. (1988) – *Empirical formulas of SPT blow-counts for gravelly soils*. Proc. ISOPT-1, Orlando, USA.

Analisi numeriche cicliche per la Cattedrale di Noto: modellazione dell'interazione terreno-struttura

Sommario

In un paese come l'Italia, caratterizzato da un elevato rischio sismico e da un enorme retaggio culturale, è di grande importanza preservare i monumenti storici dagli effetti di eventi sismici. Come ben noto, la sicurezza sismica di queste strutture viene normalmente valutata trascurando l'interazione terreno-struttura, che può invece giocare un importante ruolo. L'intento del presente lavoro consiste nell'introdurre un approccio semplificato per tenere numericamente in considerazione questo aspetto. L'interazione terreno-struttura in condizioni cicliche è tenuta in considerazione intendendo la fondazione come un macro-elemento, la cui risposta meccanica è descritta da una relazione costitutiva elastica-ipoplastica. Il modello include un incrudimento isotropo e cinematico e i suoi parametri costitutivi sono stati calibrati riferendosi a terreni granulari. Si mostra come l'implementazione numerica di detto modello in un codice FEM permetta di riprodurre realisticamente la risposta meccanica di una sezione trasversale 2-D della cattedrale di Noto.

In particolare, si è messo in luce il benefico effetto delle barre che collegano tra loro le fondazioni. Si mostra, inoltre, che l'accumulo ciclico dei cedimenti verticali sotto l'azione di un forte terremoto può portare a collasso la struttura a causa della ridistribuzione delle forze in fondazione.